EFDA–JET–CP(07)06-08

V.V. Plyusnin, M.F. Johnson, B. Alper, R. Felton, V.J. Mlynar
and JET EFDA contributors

Critical Issues Addressed to Runaway Electron Generation Expected at Major Disruptions in Reactor-Scale Tokamaks

Critical Issues Addressed to Runaway Electron Generation Expected at Major Disruptions in Reactor-Scale Tokamaks

V.V. Plyusnin[1], M.F. Johnson[2], B. Alper[2], R. Felton[2], V.J. Mlynar[3]
and JET EFDA contributors*

JET-EFDA, Culham Science Centre, OX14 3DB, Abingdon, UK

[1]Association Euratom-IST, Centro de Fusão Nuclear, Lisbon, Portugal
[2]EURATOM-UKAEA Fusion Association, Culham Science Centre, OX14 3DB, Abingdon, OXON, UK
[3]Association Euratom - IPP.CR, Prague, Czech Republic
** See annex of M.L. Watkins et al, "Overview of JET Results ",*
(Proc. 21 st IAEA Fusion Energy Conference, Chengdu, China (2006)).

Preprint of Paper to be submitted for publication in Proceedings of the
10th IAEA Technical Meeting on Energetic Particles in Magnetic Confinement Systems,
Kloster Seeon, Germany.
(8th October 2007 - 10th October 2007)

ABSTRACT.
Data on Runaway Electrons (REs) generated during major disruptions in JET has been updated. Recent studies were focused on determination of the RE current fraction during current quench and establishing generation trends toward ITER experimental parameters domain. A study of the experimental trend, which covers 1.5-6MA disruptions before and after divertor installation in JET, when the noticeable RE currents have been observed, has demonstrated the dependence of runaway process on the different character of plasma energy evolution (losses) in different type of disruptions. This is directly related to the time scale of the fast thermal quench, the theoretical basis for which is not well understood and there is no validated basis to predict the rate of plasma energy loss. Another critical point, which was considered, is associated with the influence of fast re-creation of the nested magnetic surfaces soon after reconnection and the evolution of the magnetic configuration on the behaviour of initial runaway electron population created during thermal quench. Influence of size and spatial evolution of the current-carrying channel on the dynamics of RE generation process has been studied.

1. INTRODUCTION.

With the increase of parameters of tokamak experiments toward to reactor scales major disruptions and disruption generated relativistic Runaway Electrons (REs) constitute a serious problem for safety operation of a tokamak-reactor [1, 2]. This paper presents recent advances in the study of disruption induced runaway process. The waveforms of many disruptions occurring during different stages of plasma discharges in JET have been analyzed taking into account trends toward to ITER experimental parameters domain. Significant amount of major disruptions in JET led to generation of REs with energies in the range from several MeV till to several tens of MeV and current values at the 1 MA level [3-6]. Subsequent interaction of these electrons with surrounding plasma surfaces resulted in high heat loads, melting and sputtering of the materials of the Plasma Facing Components (PFC). Comprehensive understanding of the mechanisms responsible for REs generation, their confinement and losses, is required to avoid detrimental consequences of REs in the reactor. Recent theoretical and experimental research has made important contributions to the elaboration of the model for RE generation during major disruptions in tokamaks [7-9] showing that significant fraction of pre-disruption plasma current can be converted into RE current. Note, that a majority of numerical simulation results are based on assumption that REs are generated and confined within the nested magnetic surfaces re-configured in time-scale of hundreds of microseconds after disruption reconnection [5], and which evolution is considered self-consistently without external influence. These numerical simulations allowed understanding of REs behaviour at the perfect confinement and assessment of the REs energy limits.

Major disruption is the non-uniform and non-axis-symmetric transient process. As a consequence, REs are generated in extremely non-stationary conditions. Accounting of all effects into simulation models constitutes serious problem. For example, the different character of the plasma energy loss

in various types of disruptions creates the significant difficulties in the formulation of the initial conditions for modelling. Another critical point, which was considered, is associated with mutual influence of the plasma current dynamics and RE generation process in the current quench stage. Spatial and temporal characteristics of the RE generation together with dynamics of plasma parameters during disruptions have been examined. Major disruptions and subsequent RE generation have been detected during the plasma current termination phase in JET. Analysis of these disruptions and subsequent runaway process didn't reveal strong differences in their characteristics from other runaway related disruptions. This means that for the safety ITER operations the discharge scenario should include certain procedures to avoid disruptions during termination stage of the discharge.'

2. PLASMA CURRENT DYNAMICS AND GENERATION OF RUNAWAY ELECTRON CURRENTS IN DISRUPTIONS

Presented studies were focused on determination of the RE current fraction during plasma current quench at disruptions and establishing RE generation trends toward ITER experimental parameters domain [1,2]. Data on REs generated during major disruptions in JET [5] has been updated by calculated RE currents when quasi-stationary plateaux have not been achieved. In assumption of time-independent after-disruption plasma resistivity and inductance, the plasma current evolutions during the quench stage was represented by exponentially decayed function: $I_{pl}(t) = I_{pl}(0)*\exp(-t/\tau_{qc})$ with characteristic e-folding time $\tau_{qc} = L_p/R_p$, where $R_p = 2\pi R_0\eta_{pl}/S_p$ – plasma resistance. Plasma resistivity η_{pl} and inductance L_p are: $\eta_{pl} = \text{Const}*Z_{eff}\, f(Z_{eff})*\ln\Lambda*T_e^{-3/2}$ and $L_p = 4\pi*10^{-7}R_0\{\ln(8R_0/a_p) + l_i/2 - 2\}$.

RE currents have been calculated as a difference between total plasma currents I_{pl} and exponentially decayed ohmic current fractions I_{OH}. Figure 1 presents typical evolution of plasma parameters when RE generation has been detected at spontaneous disruption of one of the recent JET pulses. An example of the inferred RE current fraction evolution is shown in Figure 2. Sometimes exponential decay with following RE generation could be distinguished after up to 50% decrease of the plasma current under conditions of strong perturbations.

Figure 3 presents the summary on RE currents values plotted verus disrupted plasma currents in JET, which covers 1.5-6MA disruptions, and when the runaway current plateaux ($dI_{pl}/dt = 0$) and semi-plateaux ($dI_{OH}/dt < dI_{pl}/dt < 0$) have been distinguished. Data on disruption generated REs is collected for experiments with divertor (plasma cross-section area $S_p = 4.71m^2$ [1-2]) and for the original (before divertor installation, S_p was by 40% larger) plasma cross-sections in JET [3]. This data demonstrates upper bound for current conversion rate (thermal plasma current into generated RE current) at the level $I_{RE}/I_{plasma} \leq 0.6$ for both cases of plasma cross-section areas [5]. Larger area of the plasma cross-section resulted in larger values of characteristic e-folding times τ_{qc} (Figure 4). The highest values of τ_{qc} in JET with divertor have been obtained when the limiter configurations have been used in experiments on disruption generated REs or at the plasma current increase stage before X-point formation. These values of τ_{qc} are close to lowest values inferred for JET experiments before the divertor installation.

ITER operation scenarios (9MA ≤ I_{pl} ≤ 15MA and toroidal magnetic field 6 T) will require significant efforts on discharge start-up optimization and plasma control for avoiding (prevention) of disruptions [1, 2]. It is obvious, that such high currents will require significantly larger termination time, during of which the disruption and generation of REs, similarly to that presented in Figure 5, are possible. Several similar disruptions, with some of them resulted in RE generation, have been observed in JET operating at high currents without and with divertor (last disruption was at 3MA current termination stage of the Pulse No: 70440, 1MA disrupted, no REs). This fact urges further developments and implementation of safety scenarios of the plasma current termination in ITER.

3. NUMERICAL MODEL FOR RUNAWAY GENERATION SIMULATIONS.

Abrupt loss of the plasma energy in a very short time and large resistive electric fields occurring in disruptions can cause the primary RE generation. Gaining very high energies the primary REs inevitably will serve as a seed population for the secondary avalanching process [10, 11]. The interaction between these two mechanisms is been studied using numerical modelling in frame of a test particle model [12, also 5-6]. A set of equations (1)-(3) has been solved at the initial conditions inferred from the experimental data (plasma current, density, etc.) or reasonably assumed plasma parameters (temperature, Z_{eff}, etc) [13] close to the experimental data in JET. The evolution of electric field in the plasma has been modelled taking into account decrease of the plasma resistive properties with the appearance of RE current and that the plasma current decays exponentially during disruption with the characteristic *e*-folding time $\tau_{cq} = I_p*(dI_p/dt)^{-1} \equiv aL_p/R_p$. For simplicity, it was assumed that REs are perfectly confined ($\tau_{RE} \to \infty$).

$$\frac{dP_{\|}}{dt} = \frac{e_c}{m_e c} E_{\|} - \frac{e^4 n_e \ln\Lambda}{4\pi\varepsilon_0^2 m_e^2 c^3}\gamma(\gamma+\alpha)\frac{P_{\|}}{P^3} - \frac{e^4 n_e \ln\Lambda}{4\pi\varepsilon_0^2 m_e^2 c^3}\frac{2B_0^2\varepsilon_0}{3m_e n_e \ln\Lambda}\left(\frac{m_e^2c^2}{e^2B_0^2R_0^2} + \frac{P_{\perp}^2}{P^4}\right)\gamma^4\beta^3\frac{P_{\|}}{P} \qquad (1)$$

$$\frac{dP}{dt} = \frac{e}{m_e c} E_{\|}\frac{P_{\|}}{P} - \frac{e^4 n_e \ln\Lambda}{4\pi\varepsilon_0^2 m_e^2 c^3}\frac{\gamma^2}{P^2} - \frac{e^4 n_e \ln\Lambda}{4\pi\varepsilon_0^2 m_e^2 c^3}\frac{2B_0^2\varepsilon_0}{3m_e n_e \ln\Lambda}\left(\frac{m_e^2c^2}{e^2B_0^2R_0^2} + \frac{P_{\perp}^2}{P^4}\right)\gamma^4\beta^3 \qquad (2)$$

$$\frac{dn_{RE}}{dt} = \lambda_R - \frac{n_{RE}}{\tau_{RE}} + \frac{n_{RE}}{t_0} \qquad (3)$$

Where $\alpha = Z_{eff} + 1$, λ_R – is the conventional primary runaway generation rate, $P_{\|}$, $P_{\perp}$, P – are the parallel, perpendicular and total electron momentum normalized to $m_e c$, $P^2 = \gamma^2 - 1$, γ – is the relativistic factor, B_0 – is the toroidal magnetic field, R_0 – is the plasma major radius,–n_{RE} – is the density of runaway electrons, $E_{DR} = e^3 ln\Lambda n_e Z_{eff}/4\pi\varepsilon_0^2 T_e$ – is the Dreicer field, $E_{CR} = E_{DR}(T_e/m_e c^2)$, $\varepsilon = E_{\|}/E_{DR}$.

$E_{\|}(t) = -\frac{L_p}{2\pi R_0}\frac{dI_p(t)}{dt} = \eta_p j_p(t)\left(1 - \frac{I_{RE}(t)}{I_p(t)}\right)$ – is the evolution of the parallel electric field,

$t_0 = \frac{4\pi\varepsilon_0^2 m_e^2 c^3}{e^4 n_e} \sqrt{\frac{3}{\pi}(Z_{eff}+5)(\frac{E_{||}}{E_{CR}}-1)^{-1}}$ – is the secondary avalanching growth characteristic time.

The evolution of the beam geometry inevitably will influence on the RE parameters, since the variation of ratio between the RE current and resistive fraction of plasma current will change the evolution of toroidal electric field $E_{||}$ due to current substitution effect. Yet another crucial effect was found at the analysis of the disruption evolution and its influence on RE generation process.

4. DISRUPTION PHENOMENOLOGY AND GENERATION OF RUNAWAY ELECTRONS.

The dynamics of disruptions with RE generation has been studied using soft X-ray tomography reconstruction and plasma imaging. Observed events have been linked to evolution of the measured plasma parameters. REs are predominantly generated at disruptions, when an extremely fast plasma energy collapse and quick relaxation of the magnetic perturbations were observed (for example, JET Pulse No: 54047 in Figure 6). RE generation has not been observed in Pulse No: 54048, in which a massive helium puff was used. It is known [14], that helium is characterized by the lowest cooling rate in comparison to other noble gases. It seems that combined effect of low plasma-cooling rate, long-lasting magnetic perturbations and slow current quench resulted in the absence of REs in Pulse No: 54048.

Detailed study of the tomography reconstruction shows that REs are generated at different scenarios of the disruption evolution. The first type of evolution can be described as following: nested magnetic surfaces are re-configured in a time-scale of hundreds of microseconds after reconnection ('hot' core, tomography reconstruction of Pulse No: 53790 in [5]), thus providing confining conditions for seeding population of REs generated during the thermal quench [9, 15]. Figure 7 presents another type of disruption dynamics (Pulse No: 54047). In this disruption the large 'hot' island is created around of cold core (this time point is shown by arrow in Figure 6, Pulse No: 54047). RE current plateau has been observed (Figure 8). However, it is not clear, how such configuration (large''hot' island and 'cold' core) develops in the future resulting in RE current plateau and how existing models can reproduce this process [7,8]. Since the disruption is non-uniform and non-axis-symmetric transient process [1, 2], another critical point, which is considered in this study, is associated with the influence of external processes on the dynamics of the RE generation. Detailed examination of the experimental waveforms shows that the RE generation is significantly decreased (or even absent) at the disruption stage when plasma current derivative achieved maximum values. Appearance of the RE current is usually detected significantly later in comparison to the results of predictive axis-symmetric numerical simulations [7-8]. Experimental curves show that transition of the plasma current decay into characteristic RE current plateau appears just at the end of plasma column inward move, which is obviously caused by the plasma pressure loss during disruptions (Figure 8). Significant differences in the dynamics of the plasma column move resulted in the different values of RE plateaux and characteristic e-folding times τ_{qc}. Model for RE generation proposed in [16] discusses the influence

of the plasma inward move onto generation process, but its validity is still to be confirmed.

Figure 9 presents the experimental curves and the curves corresponding to parameters of RE generation evaluated on the basis of Dreicer and secondary avalanching processes at the given plasma parameters evolution and constant electron temperature T_e = 8eV. In this figure the RE generation process represented by red curve (I_{REcalc}) reveals very close evolution (qualitative and quantitative) to results of [7, 8]. The same fast increase due to the primary RE generation and further growth due to secondary avalanching are obtained. However, strong difference in temporal evolutions of the calculated and observed RE generation processes is still unclear.

The changes in the initial conditions, for example, initial value of the cross-section area of the current-carrying channel or the density of seeding RE population born in thermal quench [9,15], significantly affect the final energy, density and currents of REs. Plasma imaging diagnostics and soft X-ray data [3,5] have provided important information for determination of the cross-section size of RE beams and for study how the RE beam is evolving in space and time and to locate the places of RE beam interaction with PFC in JET (Figure 10). Comparison of the plasma column inward move after magnetic flux reconnected and corresponding times and characteristics of RE generation shows that limitation of runaway current values is caused by smaller area of the current-carrying cross-section own by closer position of the centre of plasma toroidal column to the inboard PFC.

The dependence of RE generation parameters vs. initial area of the current-carrying cross-section is presented in Figure 11. Post-disruption electron temperature values ($T_e \cong 5$ - 15eV) have been inferred from the known *e*-folding times at the given plasma inductance $L_p \cong 5 \cdot 10^{-6}$ H [3]. Simulations have been carried out at chosen $T_e \cong 10$eV. RE current densities could achieve values $j_{RE} \geq 1\text{MA/m}^2$ inferred from the calculated n_{RE} with the dominating population of REs caused by the avalanching process. As it was expected, the only primary (Dreicer) mechanism of RE generation resulted in significantly higher energy of REs in comparison to the avalanching process [3, 5-7, 13].

5. ISSUES FROM JET DATA ANALYSIS TOWARDS TO ITER OPERATION DOMAIN

The data on RE generation in JET has been re-arranged with update from disruptions with non-stationary RE currents. Using the approach for disruption database analysis [1-2], all known events of the noticeable RE currents were plotted in diagrams, which allowed establishing links between JET data domain and projections for ITER. In this analysis characteristic e-folding time has been used for calculation of the current quench time $t_{qc} = 5/3(t_{80\%} - t_{20\%})$ [1-2], i.e. difference between time points in which decaying current has value of 80% fraction of its pre-disruptive value and 20% respectively. In assumption of the exponential decay the values of τ_{qc} and t_{qc} are linked by the ratio $t_{qc} = \tau_{qc}\, ln4 \approx 1.3863 * \tau_{qc}$. Figure 11(a) presents the data for the characteristic e-folding times normalized onto plasma cross-section versus disrupted currents in JET. As it is expected, this data corresponds to the disruption data domain in JET above to the recommended lower boundary 1.67ms/m^2 [1-2] of the current decay in ITER. Plotting this data versus plasma current density (Figure 11(b)) one can obtain the evidence that almost all runaway generation events well fitted

into projected domain of plasma current densities in ITER ($300kA/m^2 \le j_{pl} \le 900kA/m^2$). Yet another interesting trend for RE generation process can be found examining JET data. The updated dependence of the current conversion rate (I_{REmax}/I_{pl}) vs. characteristic e-folding time of the quenching currents (Figure 12) is demonstrating obvious increasing trend with τ_{qc} for both limiter and divertor configurations in JET.

SUMMARY

Data on runaway electrons generated during major disruptions in JET has been updated. Increasing trends in RE generation efficiency towards to ITER experimental domain have been found for whole range of the projected plasma currents in ITER. Major disruptions and subsequent RE generation have been detected during the plasma current termination phase in JET. Analysis of these disruptions and subsequent runaway process didn't reveal strong differences in their characteristics from other runaway related disruptions. This observation urges further developments and implementation of safety scenarios of the plasma current termination in ITER. Layer-like and filamentary-like structures of runaway electron beam have been observed. The changes in the initial conditions, for example, initial value of the cross-section area of the current-carrying channel or the density of seeding RE population born in thermal quench, significantly affect the final energy, density and currents of runaway electrons. Numerical simulations of the RE generation process during disruptions performed in frames of a test particle model have shown strong dependence of the runaway process on the runaway beam geometry evolution. Despite substantial decrease of the RE density the increase of the beam cross-section resulted in large RE currents reaching current conversion rates up to 0.8. Observed significant delay in detection of RE currents in experiment indicates the necessity for detailed investigation of the mechanisms responsible for RE losses and implementation of these processes into numerical models.

ACKNOWLEDGEMENTS

Authors would express their sincere gratitude to R.D. Gill, V. Riccardo, R. Jaspers, F. Salzedas, V.G. Kiptily, E. de La Luna, F. Sartori, M. R. de Baar, R. J. Buttery, P. Helander, R. J. Hastie, T.C. Hender, S. Popovichev, D. McDonald and to all members of the JET experimental team for their efforts on preparation and accomplishment of the experiments, and for the valuable support in experimental data analysis and numerical modelling.

This work has been carried out in the frame of the European Fusion Development Agreement and in frame of the Contract of Association between the European Atomic Energy Community and Instituto Superior Técnico (IST) and of the Contract of Associated Laboratory between Fundação para a Ciência e Tecnologia (FCT) and IST. The content of the publication is the sole responsibility of the authors and it does not necessarily represent the views of the Commission of the European Union or FCT or their services.

REFERENCES.

[1]. ITER Physics Basis, Nuclear Fusion **39** (1999) 2137-2638

[2]. Progress in the ITER Physics Basis, Nuclear Fusion **47** (2007) S128-S202

[3]. J. Wesson, R. D. Gill, M. Hugon et al. Nuclear Fusion **29** (1989) 641

[4]. R.D. Gill et al. Nuclear Fusion **42** (2002) 1039

[5]. V.V. Plyusnin et al. Nuclear Fusion **46** (2006) 277

[6]. V.V. Plyusnin et al. Study of runaway electron generation process during major disrupt-tions in JET. Fusion Energy 2004 (Proc. 20th Int. Conf., Vilamoura 2004) (Vienna:IAEA) CD-ROM file EX/P2-27 and http://www-naweb.iaea.org/napc/physics/fec/fec2004/index.html/

[7]. P. Helander et al. Physics of Plasmas, **11** (2004) 5704

[8]. P. Helander et al. Plasma Phys. Control. Fusion **44** (2002) B247–B262

[9]. H. Smith et al. Phys. of Plasmas **12** (2005) 122505–

[10]. Yu. A. Sokolov. JETP Letters **29** (1979) 218

[11]. M.N. Rosenbluth and S. V. Putvinski. Nuclear Fusion **37** (1997) 1355

[12]. B. Esposito et al. Physics of Plasmas **6** (1999) 238-252

[13]. D.G. White et al. Physics of Plasmas, **7** (2000) 4052

[14]. M. Bakhtiary, R. Yoshino, Y. Nishida. Fusion Science and Technology, **41** (2002) 77-88

[15]. V.V. Plyusnin et al. Plasma Phys. Contr. Fusion **44** (2002) 2021–2031

[16]. A.J. Russo, R.B. Campbell. Nuclear Fusion **33** (1993)1305

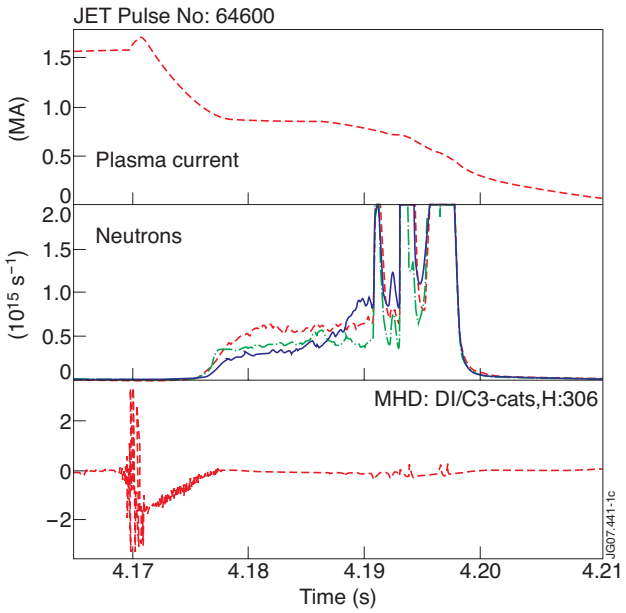

Figure 1: Typical evolution of the plasma parameters with observed RE generation at the disruption of JET pulse Pulse No: 64600

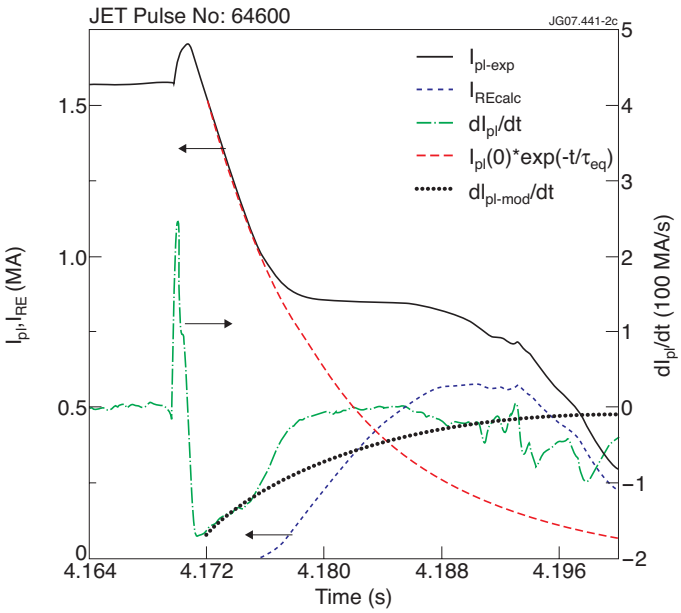

Figure 2: Calculation of the RE current fraction in assumption of time-independent after-disruption plasma resistivity and inductance and exponential plasma current decay

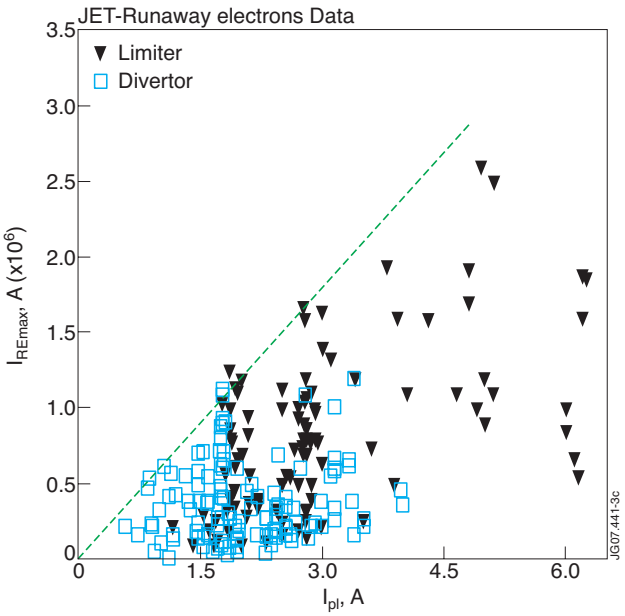

Figure 3: Summary on RE current values generated at major disruptions in JET

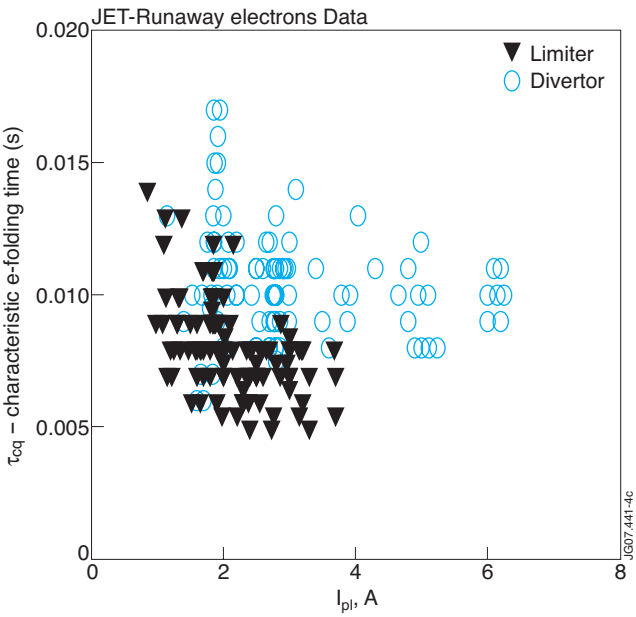

Figure 4: JET data on characteristic e-folding times of the plasma current decays plotted vs. disrupted currents at different values of plasma cross-section areas.

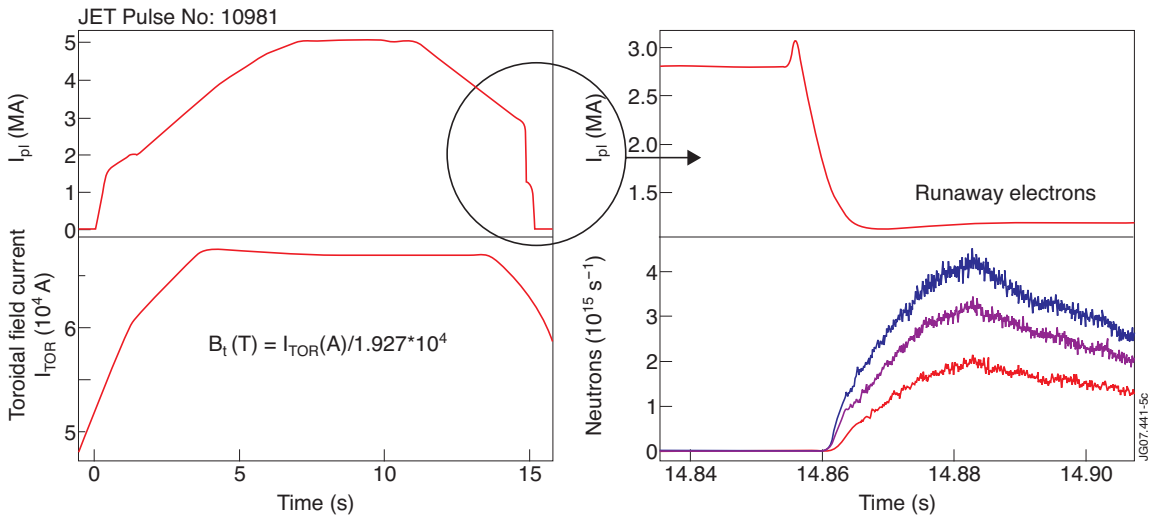

Figure 5: RE generation at the disruption of JET Pulse No: 10981 during current termination stage

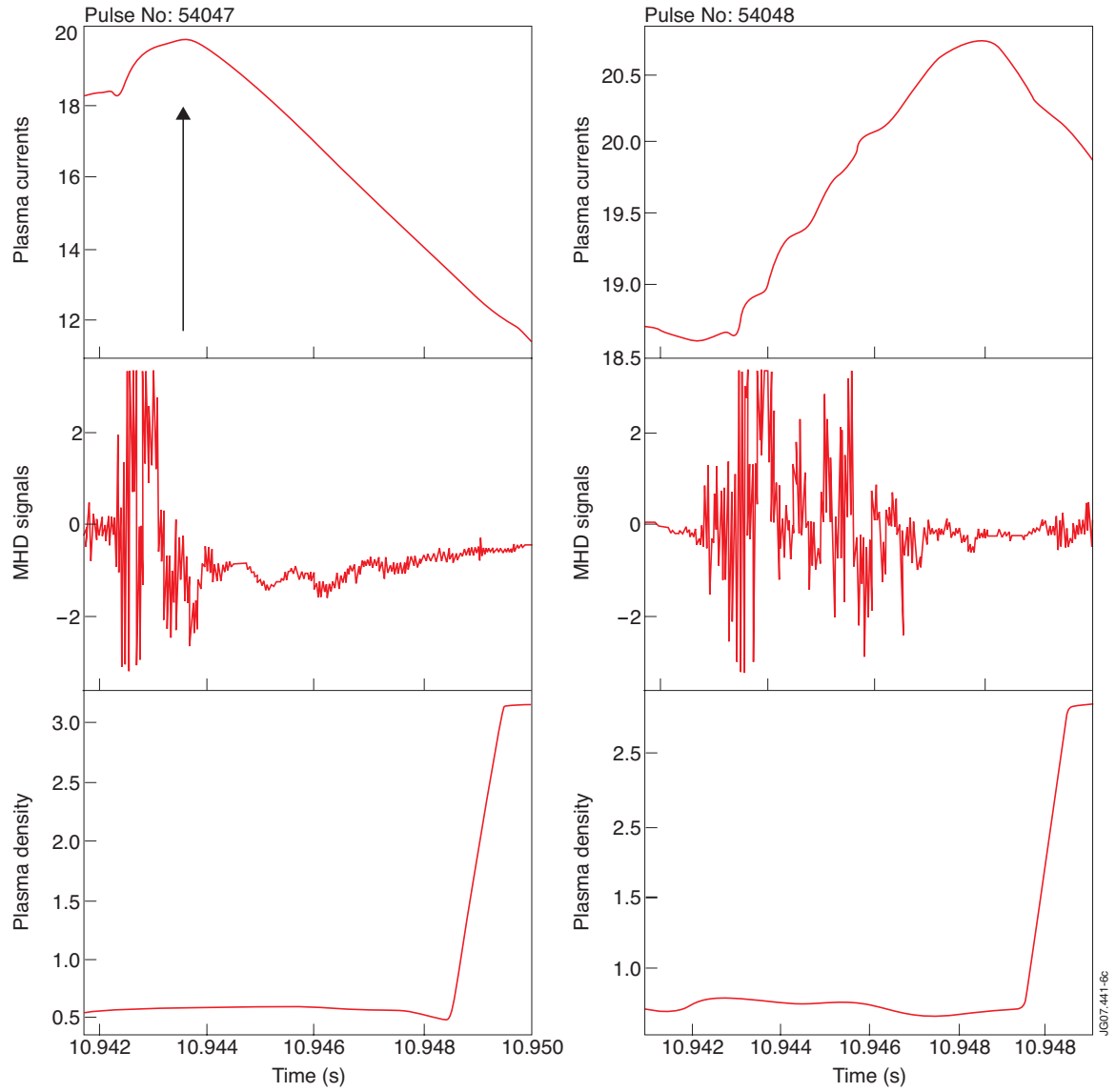

Figure 6: Examples of the 'fast' and''slow' relaxation processes in disruptions Pulse No's: 54047 and 54048 plotted in the same time-scale.

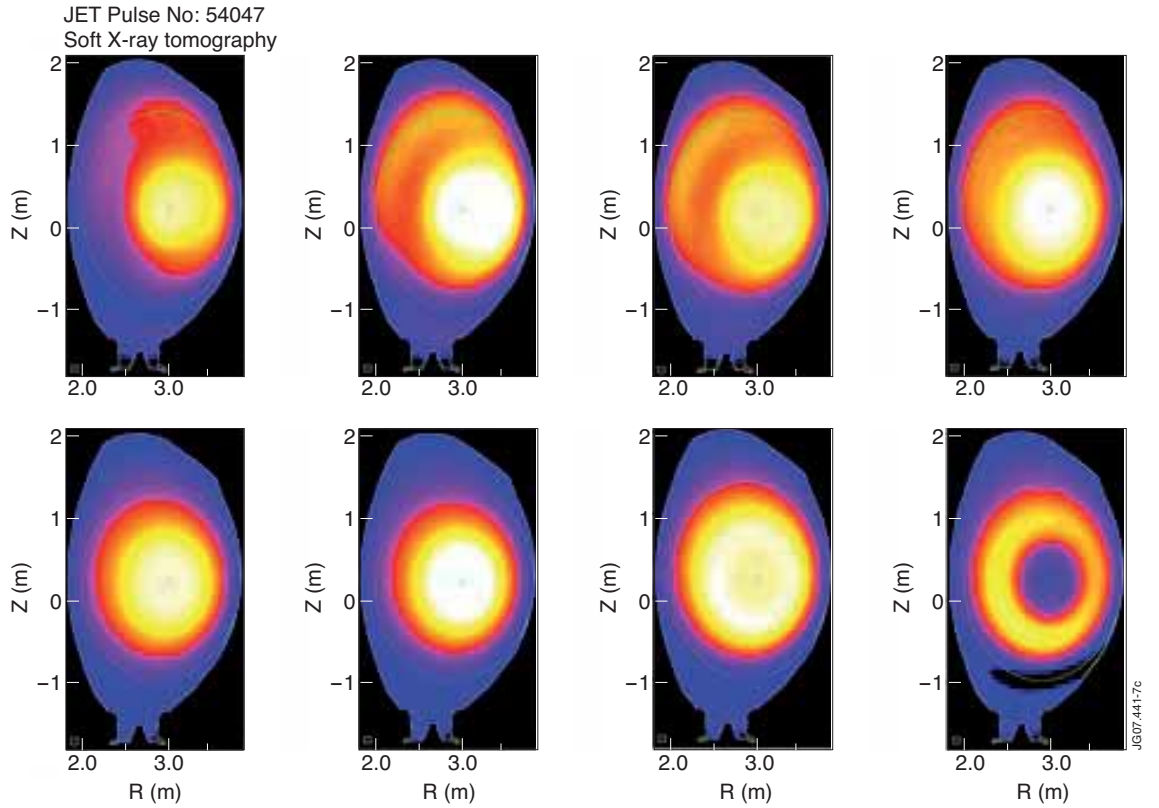

Figure 7: Soft X-ray tomography of the disruption resulted in RE generation. Last image corresponds to the temporal point marked by arrow in Figure 5.

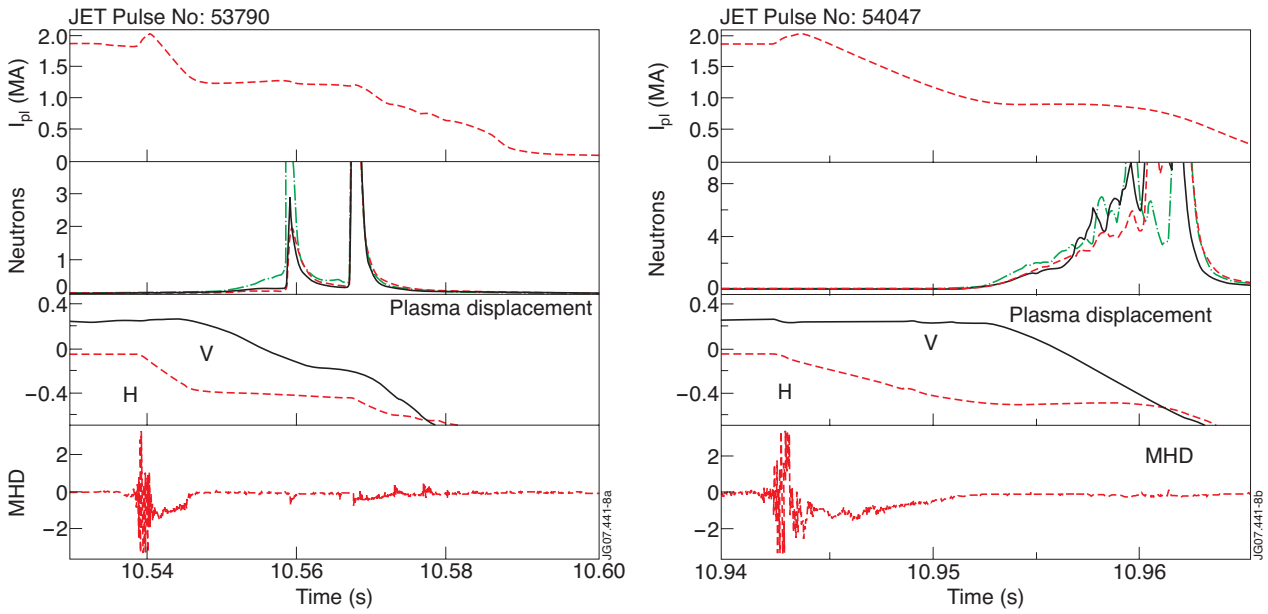

Figure 8: RE generation at the different plasma column dynamics after disruption reconnection in JET disruptive Pulse No's: 53790 and 54047, H - horizontal and V - vertical plasma displacements, respectively.

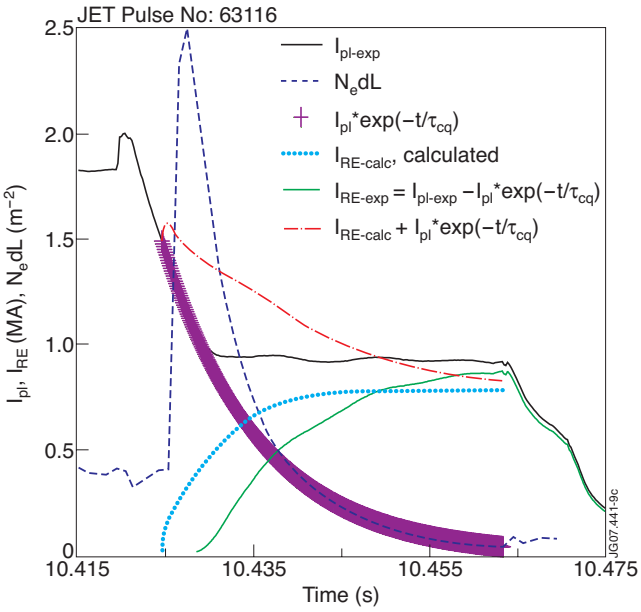

Figure 9: Comparison of the measured plasma parameters to calculated parameters of RE generation evaluated on the basis of Dreicer and secondary avalanching processes.

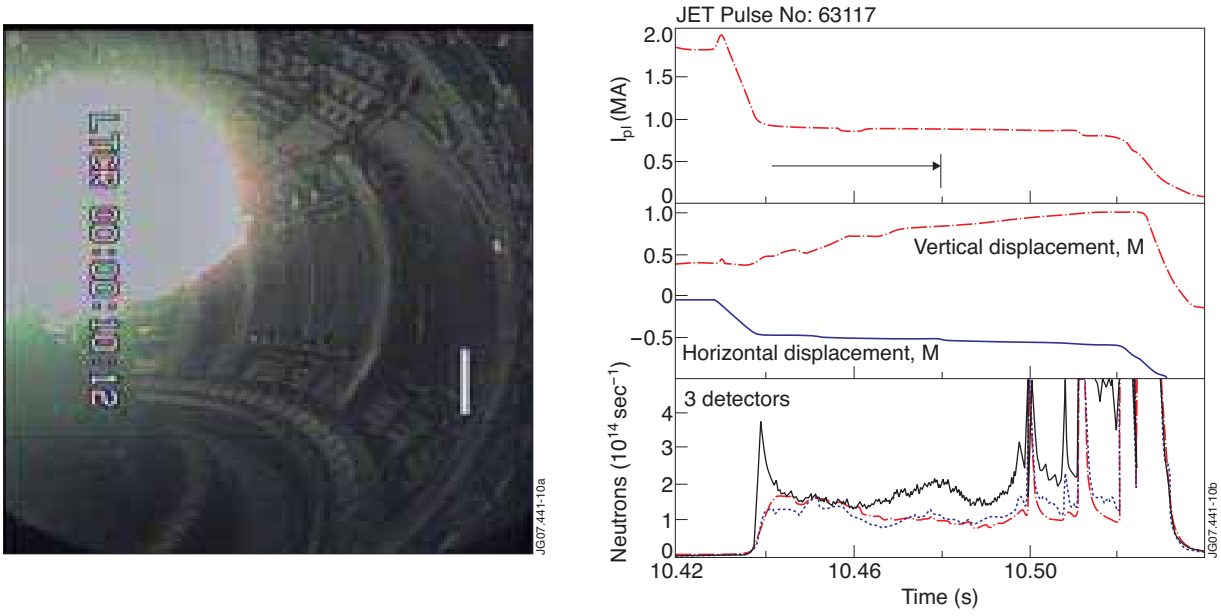

Figure 10: Example of plasma imaging data during RE generation in JET disruption Pulse No: 63117 and comparison to evolution of plasma displacement data

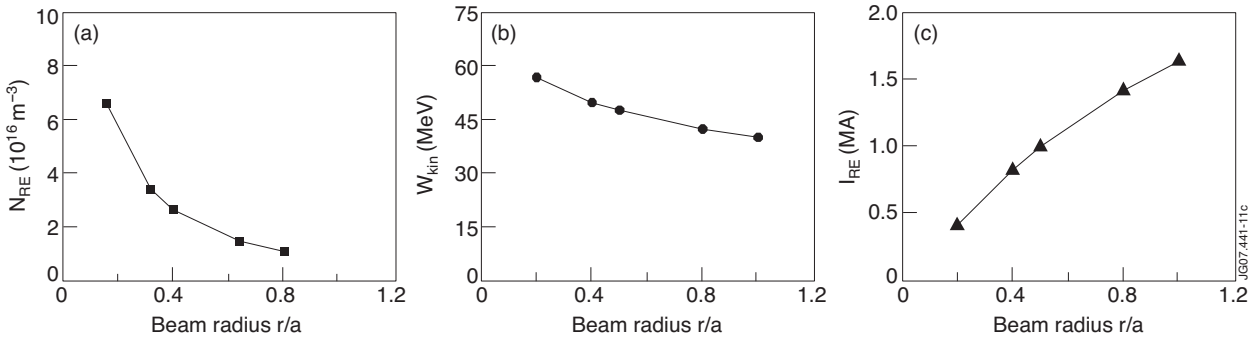

Figure 11: Dependence of the calculated RE density (a), maximal kinetic energy (b), and RE currents versus runaway beam radius.

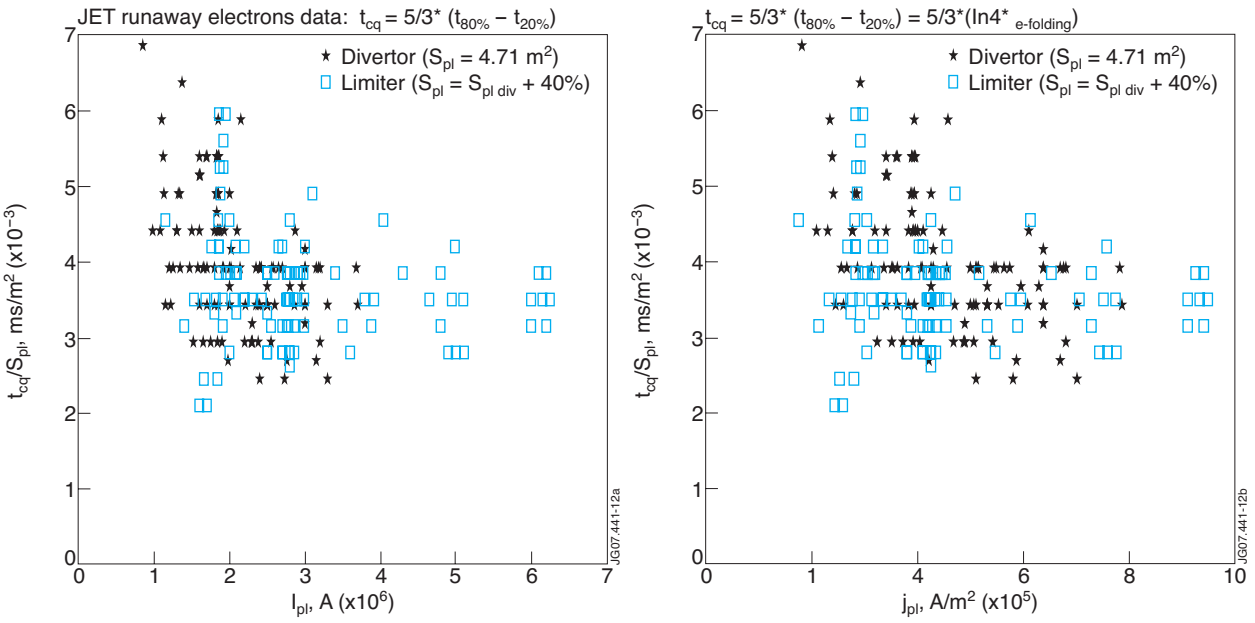

Figure 12. Dependence of the current quench time t_{qc} = 5/3($t_{80\%}$ – $t_{20\%}$) normalized on the area of the plasma cross-section in JET versus plasma current (chart A) and plasma current density (chart B) in JET experiments.

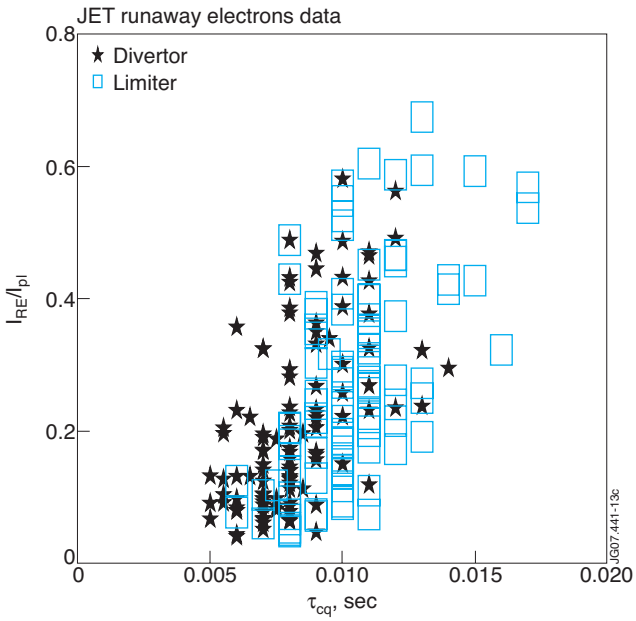

Figure 13: JET data on the currentconversion rate obtained in experimentswith divertor and limiter configurationsand plotted versus characteristic e-folding timeof the plasma decaying currents